IEEE Access
Multidisciplinary | Rapid Review | Open Access Journal

Received April 23, 2021, accepted May 17, 2021, date of publication May 24, 2021, date of current version June 1, 2021.

Digital Object Identifier 10.1109/ACCESS.2021.3082925

Displacement Estimation of Self-Sensing Magnetic Bearings Based on Biorthogonal Spline Wavelet

HAOJIE XIONG, JUN XIAO, DONGSHENG YANG, (Senior Member, IEEE), BOWEN ZHOU, (Member, IEEE), AND XIAOTING GAO, (Graduate Student Member, IEEE)
College of Information Science and Engineering, Northeastern University, Shenyang 110819, China

Corresponding author: Dongsheng Yang (yangdongsheng@mail.neu.edu.cn)

This work was supported by the National Natural Science Foundation of China under Grant U1908217.

ABSTRACT By collecting the ripple current in the control coil, the self-sensing magnetic bearings can obtain rotor displacement information without a displacement sensor, which has the advantages of low cost and high integration. According to the problems of incomplete and inaccurate displacement information extraction caused by the traditional displacement estimation method using Fourier method to analyze the ripple current with non-stationary characteristics to estimate the rotor displacement with the Gibbs effect. Therefore, this paper proposes a rotor displacement estimation algorithm based on multiresolution filter bank biorthogonal spline wavelet for a magnetic bearing motor based on two-level switching power amplifier. This algorithm utilizes the biorthogonal spline wavelet with the characteristics of generalized linear phase and tight support, which can accurately demodulate the ripple current in the coil and extract the displacement information in the ripple current. Therefore, it is able to overcome the Gibbs effect in the traditional Fourier analysis estimation algorithm, to reduce the influence of ripple on rotor displacement estimation, and to improve the accuracy and stability of displacement estimation. In order to verify the correctness and effectiveness of the proposed algorithm, this paper establishes a simulation model of magnetic bearing in MATLAB Simulink and designs the proposed displacement estimator. Simulation results demonstrate that the proposed algorithm has higher accuracy and better stability than traditional displacement estimation algorithms. Experimental results show that the maximum deviation rate of the displacement estimation method proposed in this paper does not exceed 1% when the radial magnetic bearing gap is 0.5 mm, which can effectively estimate the rotor displacement.

INDEX TERMS Self-sensing, magnetic bearing, spline wavelet, displacement estimator, multiresolution filter bank.

I. INTRODUCTION

Active magnetic bearings have a wide range of application prospects in high-speed rotating machinery due to their excellent characteristics such as no friction, no lubrication, low loss, and high speed [1], [2]. Active magnetic bearings use electromagnets to generate controllable electromagnetic force to levitate the rotor. The core feedback in the closed-loop control is the rotor displacement. Generally, the air gap between the magnetic bearing and the rotor is only a few hundred micrometers, and the magnetic bearing is mostly used in high-speed rotating machinery. The accurate rotor displacement is particularly important for the safe and stable operation of the active magnetic bearing system [3].

The associate editor coordinating the review of this manuscript and approving it for publication was Zhuang Xu.

The displacement of the rotor can be obtained by installing displacement sensors on each degree of freedom (DOF) of the rotor. However, due to the limitation of the magnetic bearing structure, the displacement sensors cannot coincide with the electromagnetic actuators, and its axial deviation is not conducive to the stability control of the magnetic bearing [4]. Meanwhile, for the flexible rotor control system, the displacement sensors and the electromagnetic actuators do not coincide, which lead to the different position of the measurement point and the electromagnetic force implementation point, which will lead to the system instability and even collapse. In addition, high-precision displacement sensors are expensive and increase the manufacturing cost of magnetic bearings [5], [6], which is not conducive to the application of magnetic bearings in industry. In view of this, self-sensing magnetic bearing was proposed for the first time in [7]. The self-sensing magnetic bearing uses the same device to

integrate displacement collection and electromagnetic levitation excitation to avoid the problem that the sensors do not coincide with the actuators.

At present, the methods to obtain displacement from self-sensing magnetic bearings are roughly divided into three categories. The first type obtains the displacement state based on the state observer. Literature [8], [9] first proposed to establish a state observer with coil current as the input and rotor displacement as the output based on the state space model of the magnetic bearing system to realize the self-sensing operation of the voltage-controlled magnetic bearing system. Subsequently, literature [10] established a multi-input multi-output system with voltage and current as the input, and electromagnetic force and rotor displacement as the output based on single input and single output, and proposed a dual-port network state model of the magnetic bearing system, which can directly obtain the rotor displacement. Although the rotor displacement as a state variable can be directly observed by the state observer, the stability of the magnetic bearing control system is sensitive to the change of model parameters, and the control system has poor robustness [11].

The second type uses intelligent algorithms to identify displacement. Literature [12] constructed a neural network with hidden layers, and the well-trained neural network can obtain the rotor displacement. However, the artificial neural network needs offline training at first, and the quality of offline training directly determines the accuracy of online detection. However, the magnetic bearing motor is often disturbed by random current signals during operation. Thus, the parameters of offline training are difficult to be directly applied to online detection.

The third type uses magnetic bearing coils to estimate the rotor displacement. This type has been widely concerned by researchers in recent years because of its intuitive and real-time stability and online estimation. It is also a mainstream displacement estimation method for self-sensing magnetic bearings. Specific implementation techniques mainly include high-frequency small-signal injection method, differential transformer method, and nonlinear parameter estimation method. The high-frequency small-signal injection method first injects a high-frequency and small-amplitude voltage or current signal at the input end of the linear power amplifier. Then, it detects the voltage value at the output end of the coil. Finally, it calculates the equivalent impedance and inductance of the coil. Literature [13] proposed the DCM algorithm for self-sensing operation of magnetic suspension bearings based on the small signal method. Literature [14], [15] used a digital controller to realize the self-sensing operation based on the high-frequency small-signal method. However, the high-frequency and small-signal method increases hardware resources in practical applications, which makes it only suitable for low-power applications. The differential transformer method takes the bias winding in the magnetic bearing as the primary coil, the control winding as the secondary coil, the rotor as the iron core, and the signal of the switching power amplifier as the input. The rotor displacement can be obtained from the high frequency component of the voltage of the control winding. In literature [16], [17], the working principle of differential transformer method in single-DOF electromagnetic bearing system was preliminarily explored and simulated. Literature [18] adopted a set of independent windings for displacement measurement. Although the differential transformer method can achieve a stable suspension of 2-DOF without sensors, it cannot be regarded as a self-sensing technology in strict sense due to its weak autobiographical perceptual integration.

The nonlinear parameter estimation method uses the function relationship between the amplitude of the ripple current generated by the high-frequency switching of the switching power amplifier and the equivalent inductance of the coil under the condition of a constant duty cycle to estimate the real-time displacement of the rotor. Literature [19] first proposed the nonlinear parameter estimation method, which used the nonlinear demodulator to extract the high-frequency ripple component of the current signal and realized the displacement estimation of the rotor. Literature [20] proposed a duty cycle compensation strategy, which reduced the hardware complexity of self-sensing. The rotor displacement estimated by the duty cycle compensation strategy was realized in the 4-DOF radial magnetic bearing system with self-sensing operation of 0-3000 Revolutions Per Minute (RPM). However, the ripple current harmonic composition of the switching power amplifier is complicated, and the current amplitude extraction process usually contains nonlinear links, and the phase lag is serious. Literature [1] proposed a rotor displacement estimation strategy based on Hilbert transform to compensate Phase lag problem. Literature [21] used the complex Morlet wavelet to improve the low Signal Noise Ratio (SNR) of self-sensing magnetic bearing systems. However, it first used Fourier transform to analyze the ripple current and estimated the rotor displacement. The traditional nonlinear parameter method uses Fourier analysis to analyze the ripple current [22], [23], while the signal of magnetic bearing motor during operation is usually a nonstationary signal, and in the digital control system, the signal is in a discrete and discontinuous state. While Fourier analysis uses trigonometric functions to fit and decompose nonstationary signals, and the Gibbs effect exists. For sudden and violent signals with ripple current, Fourier needs to use a great deal of triangular waves to fit, and the fitting decomposition is not smooth, which will lead to incomplete extraction of rotor information and affect the accuracy and stability of rotor displacement estimation.

To solve the above-mentioned problems, this paper proposes a rotor displacement estimation algorithm based on the biorthogonal spline wavelet (BSW) of the multiresolution filter bank. The special contributions of this paper include:

- A multiresolution filter bank is designed to overcome the Gibbs effect of traditional self-sensing magnetic bearing displacement estimation method.

• The corresponding multiresolution filter bank biorthogonal spline wavelet rotor displacement estimator is designed. By selecting different finite length attenuation wavelet base expansion and translation, the multiscale refined analysis of the signal is carried out, and the information extraction of nonstationary signal ripple current and displacement estimation of self-sensing magnetic bearing are realized.

• The stability and accuracy of the algorithm proposed in this paper under different working conditions and different displacement frequencies are compared with the traditional Fourier analysis method considering the duty cycle through simulation, which verifies the superiority of the algorithm proposed in this paper.

• The actual usability and effectiveness of the algorithm proposed in this paper are verified by the magnetic bearing experimental platform.

The rest of this paper is organized as follows. Section 2 introduces the basic principles of self-sensing magnetic bearings. Section 3 introduces wavelet transform and multiresolution analysis. Section 4 constructs a magnetic bearing displacement estimator based on biorthogonal spline wavelet, and Section 5 shows simulation and experimental results, and Section 6 summarizes the conclusions of the paper.

II. BASIC PRINCIPLE OF MAGNETIC BEARING SELF-SENSING

The self-sensing magnetic bearing replaces the displacement sensor with a displacement estimator. The displacement estimator uses the effective current value and voltage value of the electromagnet to extract the rotor displacement information, as shown in Fig. 1.

In Fig. 1, $k(s)$ is the magnetic bearing controller; i is the output current of the switching power amplifier; and s is the displacement.

In order to establish a single-DOF magnetic pole mathematical model, an electromagnet with an air gap is supposed as shown in Fig. 2.

The magnetic circuit in Fig. 2 is

$$\oint \mathrm{H} \cdot ds = l_c H_c + 2sH_a = NI \tag{1}$$

where H is the total magnetic field strength; l_c is the length of the iron core; H_c is the magnetic field strength of the iron core; s is the rotor displacement; H_a is the air gap magnetic field strength; N is the number of the coil turns; and I is the coil current.

Since the magnetic flux density of the iron core and the air gap are equal, H_c and H_a in (1) are equal, and (1) can be rewritten as

$$l\frac{B}{\mu_0\mu_r} + 2s\frac{B}{\mu_0} = NI \tag{2}$$

where μ_0 is the vacuum permeability; μ_r is the relative permeability; and B is the magnetic induction intensity. From (2),

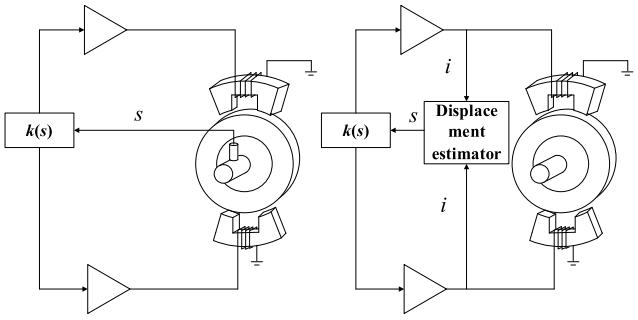

FIGURE 1. Sensor magnetic bearing and sensorless magnetic bearing.

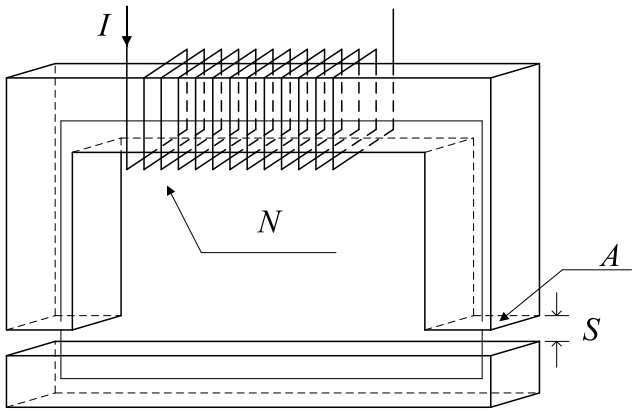

FIGURE 2. Electromagnet with air gap.

we can get

$$B = \mu_0 \frac{NI}{2s + \frac{l}{\mu_r}} \tag{3}$$

The inductance L in the magnetic circuit is the ratio of all the coil fluxes ϕ generated by a single coil in the winding to the induced current i, then

$$L = \frac{N\phi}{i} \tag{4}$$

where ϕ is the total magnetic flux generated by an N-turn coil.

The approximation calculation for the inductance in the magnetic circuit can be obtained as

$$L = \frac{\mu_0 N^2 A_a}{2s + \frac{l}{\mu_r}} \tag{5}$$

where A_a is the cross-sectional area of the air gap. Since $\mu_r \gg 1$ in the iron core, the magnetization of the iron core is usually ignored. Then, (5) can be rewritten as

$$L = \frac{\mu_0 N^2 A_a}{2s} \tag{6}$$

From (6), it can be seen that the coil inductance is inversely proportional to the air gap. Thus, it is feasible to estimate the rotor displacement by measuring the coil inductance.

The coil current driven by the magnetic bearing switching power amplifier includes effective output and high-frequency

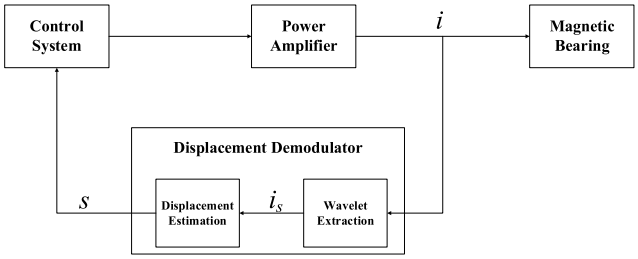

FIGURE 3. Principle of self-sensing magnetic bearings.

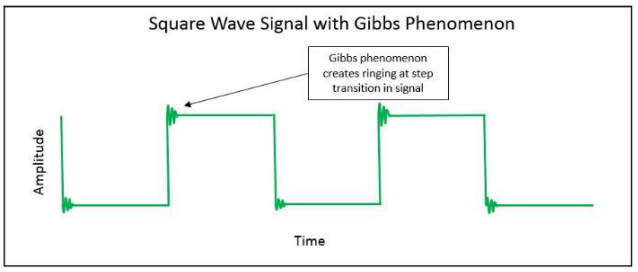

FIGURE 4. The Gibbs effect.

switching ripple. For the sake of generality, the coil current given by the switching power amplifier is

$$i = i_0 + i_s \tag{7}$$

where i is the output current of the switching power amplifier; i_0 is the effective output direct current; and i_s is the ripple current, which is generated by the high-frequency switching of the power device.

Since the magnetic bearing coil can be equivalent to inductance and resistance models, the voltage on the inductor is related to the ripple current i_s, and the voltage on the resistance is related to the total output current i.

Then the voltage applied to the electromagnet is

$$u = j\omega_s L i_s + Ri \tag{8}$$

where ω_s is the switching angle frequency, and i_s is the ripple current at the ω_s frequency.

From (8) and (6), we can get

$$i_s = \frac{2s\,(u - Ri)}{j\omega_s \mu_0 N^2 A_a} \tag{9}$$

Equation (9) is the mathematical model of magnetic bearing self-sensing. From (9), it can be concluded that the amplitude of the high-frequency ripple current i_s is related to the rotor displacement, and thus the rotor displacement related information can be obtained by extracting the amplitude of i_s.

As shown in Fig. 3, the total output current i of the power amplifier is extracted to obtain the high-frequency ripple current i_s, and i_s is demodulated to obtain the estimated rotor displacement s. The magnetic bearing control system uses the estimated rotor displacement to control the magnetic bearing.

III. SPLINE WAVELET TRANSFORM AND MULTIRESOLUTION ANALYSIS

At present, the Fourier analysis method is commonly used to analyze the coil current, and the coil voltage affected by the duty cycle is subjected to Fourier decomposition, and the corresponding fundamental frequency component of the current is extracted for operation demodulation. When the magnetic bearing motor is at operation, both the rotor displacement and ripple current change instantaneously, with strong nonstationary signal characteristics. The Fourier analysis will use a large number of triangular waves to fit the sudden and violent signal of the ripple current, that is, the signals obtained by the Fourier analysis have obvious oscillation at the turning point, as shown in Fig. 4. It will affect the accuracy and stability of displacement extraction.

The wavelet transform selects different spline functions to derive different wavelet bases, and uses finite-length attenuating wavelet base expansion and translation to perform multiscale refinement analysis on the signal. For signal nonstationary parts, only when the wavelet function does not coincide with it, the transform coefficient is not zero, which can remove the oscillation at the turning point, so it is suitable for the analysis of instantaneous nonstationary signals and overcomes the Gibbs effect [24]. Thus, it is suitable for the analysis of instantaneous nonstationary signals.

A. SPLINE WAVELET TRANSFORM

The spline function is often used in curve fitting, which has simple form, compact support set, first order vanishing moment, and generalized linear phase. Both the fitted curve and its derivative are smooth. However, the spline function is a low-pass function, which cannot be used as wavelet. When extracting the amplitude of the high-frequency component of the ripple current of the magnetic bearing, a wavelet with a band-pass property is required for preliminary processing of the current signal. Therefore, a spline wavelet with a band-pass property needs to be derived through a spline function. In this paper, the required wavelet is derived through the quadratic spline function.

The quadratic spline function is

$$\theta(t) = \begin{cases} \frac{1}{2}t^2 & 0 \le t < 1 \\ \frac{3}{4} - (t - \frac{3}{2})^2 & 1 \le t < 2 \\ \frac{1}{2}(t-3)^2 & 2 \le t < 3 \\ 0 & \text{else} \end{cases} \tag{10}$$

The frequency domain expression is

$$\Phi(\omega) = e^{-j\frac{3}{2}\omega}[\frac{\sin\frac{\omega}{2}}{\frac{\omega}{2}}]^3 \tag{11}$$

where $\Phi(\omega)$ is the spline wavelet function.

If $x(t)$ is a square integrable function and there is a function $\Phi(t)$ such that $c_\psi = \int_{-\infty}^{\infty} \frac{|\Phi(\omega)|^2}{\omega} d\omega < \infty$, the spline wavelet

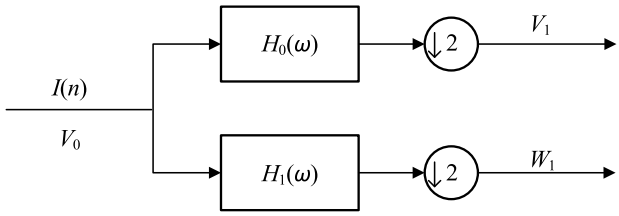

FIGURE 5. Band allocation.

transform of $x(t)$ is defined as

$$WT_x(a,\tau) = \frac{1}{\sqrt{a}}\int x(t)\Phi^*(\frac{t-\tau}{a})dt = \langle x(t), \Phi_{a\tau}(t)\rangle \quad (12)$$

where a is the scale factor; τ is the displacement; Φ is the spline wavelet; $\Phi_{a\tau}(t) = \frac{1}{\sqrt{a}}\Phi(\frac{t-\tau}{a})$ is the displacement and scale expansion of the spline wavelet. In (12), t, a, and τ are all continuous variables, and thus (12) is also called continuous spline wavelet transform. The equivalent frequency domain of (12) is expressed as

$$WT_x(a,\tau) = \frac{\sqrt{a}}{2\pi}\int X(\omega)\Phi^*(a\omega)e^{j\omega t}d\omega \quad (13)$$

From (13), it can be seen that if $\Phi(\omega)$ is a bandpass function with relatively concentrated amplitude-frequency characteristics, the spline wavelet transform has the ability to characterize the local properties of the signal $X(\omega)$ in the frequency domain, and different scale factors will not change its quality factor. Therefore, from the point of view of the frequency domain, using spline wavelet transform at different scales to process the signal is similar to using a set of band-pass filters to process the signal.

B. MULTIRESOLUTION ANALYSIS OF CURRENT SIGNAL

In wavelet transform, when the scale factor a is large, a general observation is acceptable, and when the scale factor a is small, a detailed observation is required. The quality factor of different scale factor analysis remains unchanged and this kind of gradual analysis from rough to precise is called multiresolution analysis. In the actual operation of the magnetic bearing system, the coil current data sampled by the processor through Analog to Digital (A/D) are a discrete sequence. Thus, the discrete sequence $I(n)$ is directly used as the input in this paper, and the whole calculation process is achieved in a discrete state.

Fig. 5 shows the multiresolution frequency band division.

In Fig. 5, $I(n)$ is the discrete sequence of coil current signals, and $H_0(\omega)$ and $H_1(\omega)$ are low-pass filters and high-pass filters derived from spline wavelets.

If the total frequency band $(0 \sim \pi)$ occupied by the high-frequency current $I(n)$ is defined as the space V_0, it is decomposed into two subspaces through the first level: low-frequency V_1 and high-frequency W_1. The second-level decomposition can be performed on V_1 to obtain low-frequency V_2 and high-frequency W_2, and so on. According to the Nyquist theorem, the normalized frequency band is limited to between $-\pi \sim +\pi$. Then, the signal can be decomposed at this time. The ideal low-pass filter and the ideal high-pass filter are used to divide the low-frequency part and the high-frequency part. The output bandwidth is halved, and thus the sampling rate can be halved without loss of information. The decomposed low-frequency and high-frequency parts can be continuously decomposed until the required high-frequency ripple current signal frequency is decomposed to achieve the effect of multiresolution.

IV. DISPLACEMENT ESTIMATION OF MAGNETIC BEARING BASED ON BIORTHOGONAL SPLINE WAVELET

This section firstly uses spline wavelets to derive a multiresolution analysis spline wavelet filter bank; then, it designs a magnetic bearing displacement estimation algorithm based on BSW; afterwards, it extracts the high frequency ripple component of the coil current; and finally it obtains the magnetic bearing rotor displacement information.

Fig. 6 shows the flow chart of the magnetic bearing displacement estimation algorithm. The required high-frequency ripple current signal $I_s(n)$ is obtained after multilayer decomposition of the coil current $I(n)$ output by the switching power amplifier. As the BSW algorithm model is essentially a bandpass filter, the ripple current $I_s(n)$ is obtained after wavelet decomposition. Thus, the absolute value operation is added to make its output only contain positive signals, and the low-pass filter is used to attenuate all the high-frequency components to almost zero, leaving only the envelope. The envelope is the air gap length signal modulated in the high frequency component, which means that the signal containing the required displacement. The rotor displacement s can be estimated and demodulated by (9), and the displacement estimated s is sent to the magnetic bearing control algorithm for displacement adjustment.

In Fig. 6, $I(n)$ is the coil current under the discrete condition; $I_s(n)$ is the ripple current under the discrete condition; and s is the estimated rotor displacement.

Therefore, the discrete current signal $I(n)$ is decomposed and expanded by wavelets.

$$I(n) = \frac{1}{\sqrt{2}}\sum_i^\infty\sum_k^\infty C_{\varphi(i,k)}\varphi_{i,k}(n) + \frac{1}{\sqrt{2}}\sum_j^\infty\sum_k^\infty D_{\psi(j,k)}\psi_{j,k}(n) \quad (14)$$

In (14), i and j are the resolution orders, and k is the offset.

$$C_{\varphi(i,k)} = \frac{1}{\sqrt{2}}\sum_n I(n)\varphi_{i,k}(n) \quad (15)$$

$C_{\varphi(i,k)}$ is the approximate coefficient of discrete wavelet transform, and $\phi_{i,k}(\mathrm{n})$ is the scale function.

$$D_{\psi(j,k)} = \frac{1}{\sqrt{2}}\sum_n I(n)\psi_{j,k}(n) \quad (16)$$

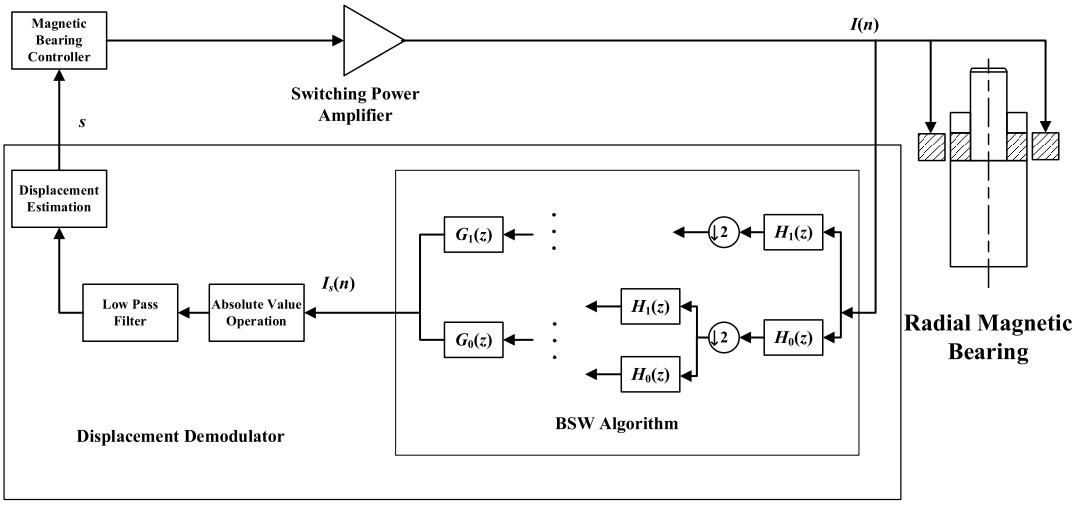

FIGURE 6. Flow chart of magnetic bearing displacement estimation algorithm.

$D_{\psi(j,k)}$ is the wavelet coefficient of discrete wavelet transform; $\psi_{j,k}(\mathrm{n})$ is the wavelet function. The different values of i and j can obtain current signals with different resolutions.

It can be seen from (8) that the inductance containing the rotor displacement is closely related to the current at the switching frequency. Thus, the ripple current signal $I_s(n)$ at the switching frequency can be obtained by taking different values of i and j. In order to obtain $I_s(n)$, the scale function $\varphi_{i,k}(\mathrm{n})$ and wavelet function $\psi_{j,k}(\mathrm{n})$ should be obtained first. The low-pass filter H_0 and the high-pass filter H_1 are derived from the multiresolution analysis filter bank, and then extract the ripple current $I_s(n)$.

In order to facilitate the calculation of wavelet transform, orthogonal wavelet is usually used to reduce the calculation amount, and when only the wavelet is orthogonal, the information contained in wavelet transform has no redundancy. However, the tightly supported orthogonal multiresolution analysis wavelet lacks symmetry and cannot be symmetric or antisymmetric, and the corresponding filter cannot maintain a linear phase. In order to overcome the shortcomings of orthogonal wavelets and construct a finite-length filter with linear phase, biorthogonal wavelets are introduced. A biorthogonal wavelet filter bank is constructed using the spline wavelet function derived above, as shown in Fig. 7.

Get the relationship from Fig. 7,

$$I_s(z) = \frac{1}{2}[H_0(z)G_0(z) + H_1(z)G_1(z)]I(z) + \frac{1}{2}[H_0(-z)G_0(z) + H_1(-z)G_1(z)]I(-z) \quad (17)$$

where $I(z)$ is the current input of the magnetic bearing coil; $I_s(z)$ is the coil current high-frequency ripple current output; $H_0(z)$ and $H_1(z)$ are the decomposed low-pass filters and high-pass filters in the discrete domain; $G_0(z)$ and $G_1(z)$ are reconstructed low-pass filters and high-pass filters in the discrete domain. $H_1(z)$ can continuously decompose the high-frequency components in the previous signal.

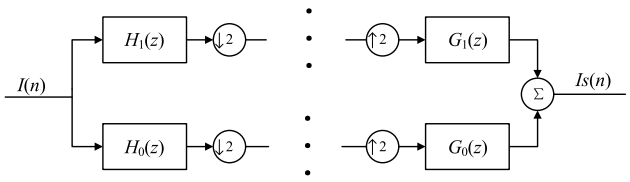

FIGURE 7. Two-channel filter bank.

In order to eliminate the aliasing caused by $I(-z)$ in (17), it is required that

$$H_0(-z)G_0(z) + H_1(-z)G_1(z) = 0 \quad (18)$$

where introduce anti-aliasing conditions

$$\begin{cases} G_0(z) = z^{-l}H_1(-z) \\ G_1(z) = -z^{-l}H_0(-z) \end{cases} \quad (19)$$

In order to make each layer of signal decomposition and output pure delay, it is required that

$$H_0(z)G_0(z) + H_1(z)G_1(z) = cz^{-k} \quad (20)$$

In this paper, $c = 1$, $k = 0$, and $l = 0$ are used to reduce the delay in extracting the rotor displacement. The low-pass filter can be obtained from the spline wavelet function in (11).

$$H_0(\omega) = \sqrt{2}\frac{\Phi(2\omega)}{\Phi(\omega)} = \sqrt{2}\, e^{-j\frac{3}{2}\omega}\cos^3\frac{\omega}{2} \quad (21)$$

(21) can be reduced to

$$H_0(\omega) = \sqrt{2}[\frac{1}{8} + \frac{3}{8}e^{-j\omega} + \frac{3}{8}e^{-j2\omega} + \frac{1}{8}e^{-j3\omega}] \quad (22)$$

Using (22) to transform in the discrete domain, the low-pass filter in the discrete domain can be obtained

$$H_0(z) = \sqrt{2}[\frac{1}{8} + \frac{3}{8}z^{-1} + \frac{3}{8}z^{-2} + \frac{1}{8}z^{-3}] \quad (23)$$

According to (19) and (20), the high-pass filter and reconstruction filter can be derived:

$$\begin{cases} H_1(z) = \sqrt{2}[-\frac{1}{8} - \frac{3}{8}z^{-1} + \frac{3}{8}z^{-2} + \frac{1}{8}z^{-3}] \\ G_0(z) = \sqrt{2}[-\frac{1}{8} + \frac{3}{8}z^{-1} + \frac{3}{8}z^{-2} - \frac{1}{8}z^{-3}] \\ G_1(z) = -\sqrt{2}[\frac{1}{8} - \frac{3}{8}z^{-1} + \frac{3}{8}z^{-2} - \frac{1}{8}z^{-3}] \end{cases} \tag{24}$$

Since the even-order terms of $H_1(z)$ and $H_1(-z)$ have changed signs, after the multiplication of $H_1(z)H_1(-z)$, there are only even-order terms and no odd-order terms, which indicates that $G_0(z)H_1(z)$ has only odd-order terms. Let the inverse transformation of $G_0(z)$ be $g_0(n)$, and the inverse transformation of $H_1(z)$ into $h_1(n)$, we can get

$$\begin{cases} g_0(n) = +(-1)^n h_1(n-1) \\ g_1(n) = -(-1)^n h_0(n-1) \end{cases} \tag{25}$$

Then the actual $g_0(n)$, $h_1(n-l)$, $g_1(n)$ and $h_0(n-l)$ have the following relationship:

When l is odd

$$\begin{cases} \left\langle g_0(n), \tilde{h}_1(n-2k) \right\rangle = 0 \\ \left\langle g_1(n), \tilde{h}_0(n-2k) \right\rangle = 0 \end{cases} \tag{26}$$

When l is even

$$\begin{cases} \left\langle g_0(n), \tilde{h}_1(n-2k+1) \right\rangle = 0 \\ \left\langle g_1(n), \tilde{h}_0(n-2k+1) \right\rangle = 0 \end{cases} \tag{27}$$

where, $\tilde{h}_1(n)$ is the timing reversal of $h_1(n)$, and $\tilde{h}_0(n)$ is the timing reversal of $h_0(n)$.

According to the biorthogonal condition of the above equations, biorthogonal wavelets can have both compact support and linear phase. The linear phase ensures that the magnetic bearing coil current signal passes through the filter bank with the same delay of each frequency component, thereby ensuring that the decomposed signal is not distorted. This is of great significance for magnetic bearing systems that require high real-time and accuracy of rotor displacement.

Selecting the appropriate A/D sampling frequency to decompose the magnetic bearing coil current $I(n)$ through the designed BSW filter group to obtain the high-frequency switching current signal, which is the required pattern containing the displacement. Wave current $I_s(n)$, after demodulating the ripple current, the rotor displacement will be obtained. Therefore, the magnetic bearing can obtain the rotor displacement without a displacement sensor.

V. SIMULATION AND EXPERIMENT

In this paper, a simulation model is built in the Matlab Simulink environment, taking a single-DOF two-level switching power amplifier magnetic bearing system as an example to verify the effectiveness and correctness of the designed BSW algorithm and displacement estimator. The built-up magnetic bearing system simulation model can simulate the coil current affected by the air gap, the relationship between magnetic bearing force and current, and the relationship between force and displacement. The effectiveness of the proposed displacement estimation strategy is also tested on the experimental platform of magnetic bearing permanent magnet synchronous motor.

A. SIMULATION MODEL ESTABLISHMENT

1) MAGNETIC BEARING SYSTEM MODEL

The magnetic bearing system is controlled by PID controller. The bus voltage is $u = 50$ V; the internal resistance of the coil is $R = 0.5\ \Omega$; the rated inductance of the coil $L_0 = 12.6$ mH; the magnetic pole area $A = 1000\ \text{mm}^2$; the number of coil turns $N = 100$; the rated air gap $s_0 = 0.5$ mm; bias current $i_0 = 3.82$ A; switching frequency $f_s = 20$ kHz. The displacement force stiffness and current force stiffness of the magnetic bearing are calculated, and the discrete transfer function is used to simulate the dynamic model of the magnetic bearing.

2) SIMULATED INDUCTOR MODEL

It can be seen from (6) that the inductance of magnetic bearing coil is affected by the size of the air gap, while the inductance element in the Matlab Simulink environment is a fixed inductance and does not change with the change of the air gap. The ripple current obtained by the simulation does not include displacement. This paper builds a module to simulate the equivalent inductance of the coil that changes with displacement.

In the continuous state, the circuit has the following relationship [25]

$$u - iR = \frac{\mu_0 N^2 A}{2(s+s_0)} \frac{di}{dt} \tag{28}$$

According to (28), a discrete simulated inductor model can be built. The input is the ripple current generated by the high-frequency switching of the power device of the magnetic bearing system, and the output is the ripple current containing the displacement.

3) WAVELET DISPLACEMENT ESTIMATOR MODEL

The BSW algorithm model and displacement estimator for multiresolution filter banks are established. Since the ripple current generated by the power amplifier contains many harmonics, the BSW algorithm also functions as a band-pass filter. According to the Nyquist theorem, a wavelet filter bank is used to extract the input signal. In this paper, the switching frequency of the switching power amplifier is 20 kHz; the system simulation sampling frequency is 200 kHz; the entire frequency is limited to $0 \sim \pi$, and the Nyquist frequency is 100 kHz as the highest frequency. After the input signal is processed by the BSW algorithm, the absolute value operation and low-pass filter are added for reprocessing.

4) FOURIER ANALYSIS ESTIMATOR MODEL CONSIDERING DUTY CYCLE

This paper establishes a Fourier analysis estimator model considering the duty cycle, extracting the real-time duty cycle and ripple current of the Pulse-Width Modulation (PWM) wave as input signals, passing through a band-pass filter [26], absolute value calculation, and low pass filter. The parameters of absolute value operation and low pass filter are consistent with the wavelet displacement estimator model, and the output is the displacement. The core calculation equation is

$$I_n = \frac{4V_s}{jn^2\pi\omega_s L}[\sin(n\pi\alpha)], \quad n = 1, 2, 3, \ldots \tag{29}$$

where I_n is the n-th switching current ripple component; V_s is the DC bus voltage; ω is the switching angular frequency; and α is the duty cycle. This paper takes $n = 1$.

B. SIMULATION ANALYSIS

1) MAGNETIC BEARING STATIC START SUSPENSION

The sampling step is 5e-6, and the displacement of the static low-pass filter at 0.5 kHz, 1 kHz, and 1.5 kHz is considered for simulation verification.

Figs. 8-10 are the displacement comparison figures.

According to Figs. 8-10, it can be seen that the BSW algorithm estimator and the Fourier analysis method considering the duty cycle can well follow the actual displacement of the magnetic bearing, whereas they all deviate from the actual displacement. With the increase of frequency, the performance of the two algorithms for estimating the rotor displacement starts unstable. In practical engineering, the magnetic bearing coil current is a nonstationary mutation signal, and the Fourier analysis method considering the duty cycle uses a trigonometric function to fit the coil current, which has the Gibbs effect. The analysis and extraction of displacement signals are not accurate, and the estimated displacement fluctuates severely under different frequency displacement. From (29), it can be seen that the fluctuation frequency is affected by the change of the duty cycle when the magnetic bearing system is adjusted. The fluctuation amplitude increases with the increase of the frequency of the displacement. In contrast, the displacement estimated by the designed BSW algorithm estimator is more stable under the three frequencies, and as the frequency of the displacement increases, the displacement estimated by the BSW algorithm estimator fluctuates to a certain extent, while the amplitude and frequency of the fluctuation are both within the acceptable range of the magnetic bearing system control.

2) STATIC SUSPENSION OF MAGNETIC BEARING UNDER DISTURBANCE

The disturbance is added when the system is operating for 0.5 s, and the disturbance amplitude is 0.02.

According to Figs. 11-13, it can be seen that under different frequencies, the Fourier analysis method considering the duty cycle and the BSW algorithm estimator are both sensitive to interference, while when the magnetic bearing control system suppresses the interference, the duty cycle is adjusted frequently, and the displacement information fluctuation estimated by the Fourier analysis method considering the duty cycle increases with the actual displacement frequency, up to 1.1 kHz. The amplitude of the fluctuation can reach 0.007 mm under 0.5 kHz displacement, 0.009 mm under 1 kHz displacement, and 0.011 mm under 1.5 kHz displacement. Such fluctuation amplitude and frequency are unacceptable for the stability control of the magnetic bearing control system, and the maximum displacement fluctuation frequency estimated by the BSW algorithm estimator is less than 250 Hz. The

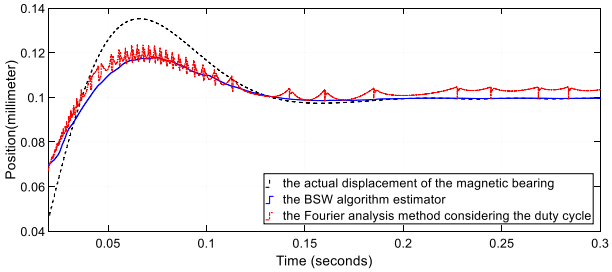

FIGURE 8. Displacement comparison at 0.5 kHz.

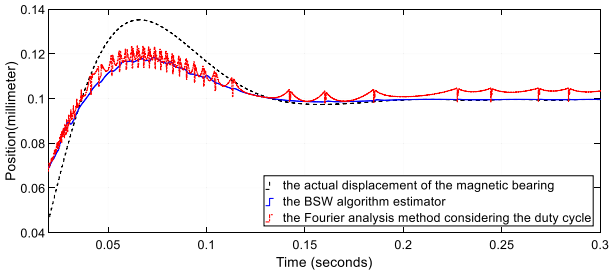

FIGURE 9. Displacement comparison at 1 kHz.

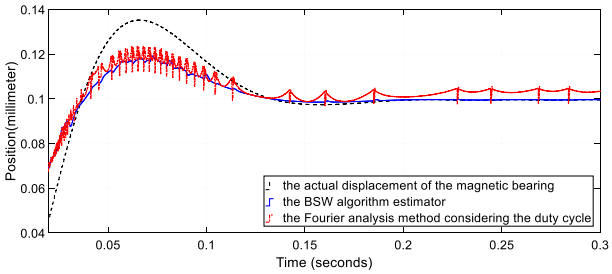

FIGURE 10. Displacement comparison at 1.5 kHz.

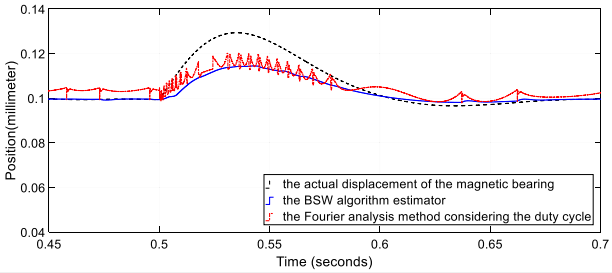

FIGURE 11. Comparison of 0.5 kHz displacement under disturbance.

TABLE 1. Performance comparison with traditional methods.

Frequency /Hz	Average Value /mm		Max Value/mm	
	Fourier analysis method considering duty cycle	BSW algorithm estimator	Fourier analysis method considering duty cycle	BSW algorithm estimator
0.5 k	0.0057	0.0032	0.0626	0.0408
1 k	0.0057	0.0036	0.0507	0.0490
1.5 k	0.0057	0.0038	0.0516	0.0525

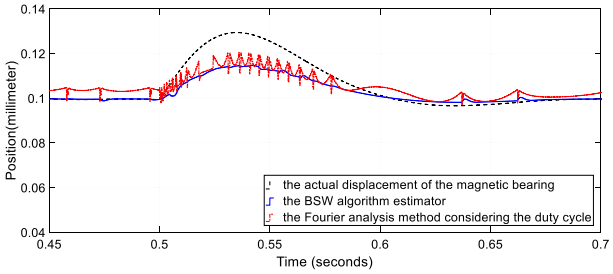

FIGURE 12. Comparison of 1 kHz displacement under disturbance.

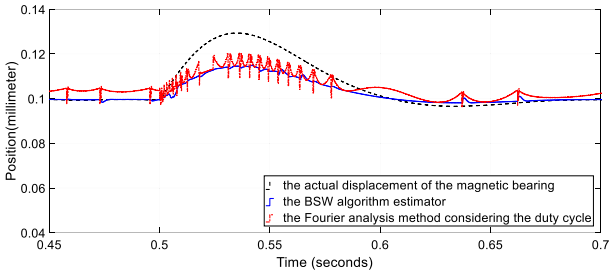

FIGURE 13. Comparison of 1.5 kHz displacement under disturbance.

maximum fluctuation amplitude is 0.0004 mm under 0.5 kHz displacement, 0.0007 mm under 1 kHz displacement, and 0.002 mm under 1.5 kHz displacement. It can be seen that the stability and accuracy of the estimated displacement of the BSW algorithm estimator are higher than that of the Fourier analysis method considering the duty cycle, and it overcomes the problem of the excessively high frequency of the estimated displacement fluctuation.

3) ALGORITHM COMPARISON UNDER STATIC SUSPENSION OF MAGNETIC BEARING

Taking the displacement deviation $e_x = x_m - x_0$, where, x_m is the displacement estimated by the self-sensing algorithm, and x_0 is the actual magnetic bearing displacement. Calculating the average and maximum values of the displacement deviation of the Fourier analysis method considering the duty cycle and the displacement deviation of the BSW algorithm estimator, respectively, and comparing and analyzing the performance of the two methods.

According to Table 1, it can be concluded that the average displacement deviation estimated by the Fourier analysis method considering the duty cycle is stable at 0.0053 mm at the three frequencies, while the average displacement deviation estimated by the BSW algorithm estimator is compared with that of the duty cycle. The Fourier analysis method reduces 38% on average, and the accuracy of estimating the displacement is higher than that of the Fourier analysis method considering the duty cycle. At 0.5 kHz displacement, the maximum displacement deviation estimated by the BSW algorithm estimator is reduced by 35% compared with the Fourier analysis method considering the duty cycle. At 1 kHz and 1.5 kHz displacement, the maximum displacement deviation estimated by the two methods is not much different. Therefore, under low-frequency displacement, the accuracy and stability of the designed BSW algorithm for estimating displacement are also better than that of the Fourier analysis method considering the duty cycle. Based on the above simulation, in the actual operation of the magnetic bearing motor, the displacement fluctuation does not exceed 1kHz, that is, the motor speed does not exceed 1kHz, the designed method can effectively estimate the actual displacement.

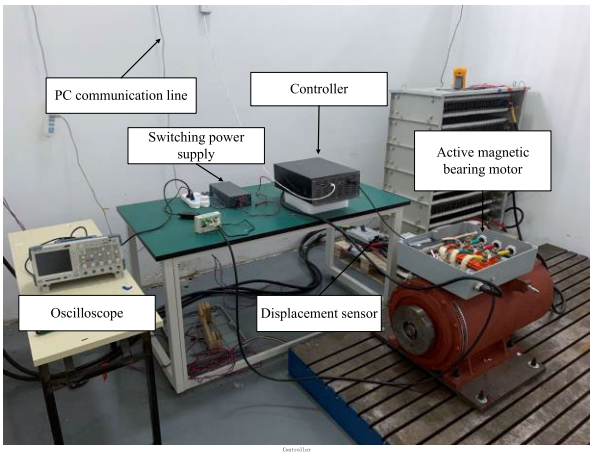

FIGURE 14. 5 degrees of freedom magnetic bearing permanent magnet synchronous motor experimental platform.

C. SUSPENSION EXPERIMENT

The designed algorithm is verified on the experimental platform of a magnetic bearing permanent magnet synchronous motor. As shown in Fig. 14, the experimental platform of 5-DOF magnetic bearing permanent magnet synchronous motor is mainly composed of magnetic bearing synchronous motor, controller and frequency converter.

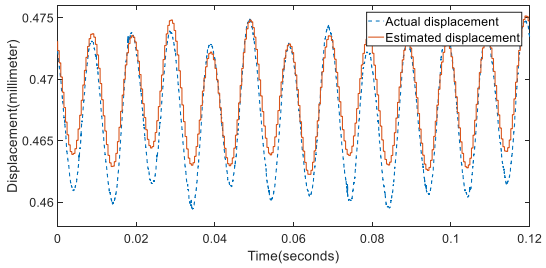

FIGURE 15. Displacement comparison of radial bearing under 100 Hz vibration.

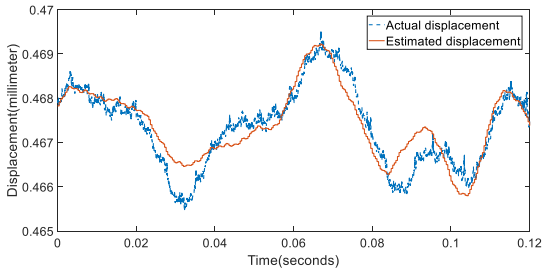

FIGURE 16. Displacement comparison of radial bearing under 500 Hz vibration.

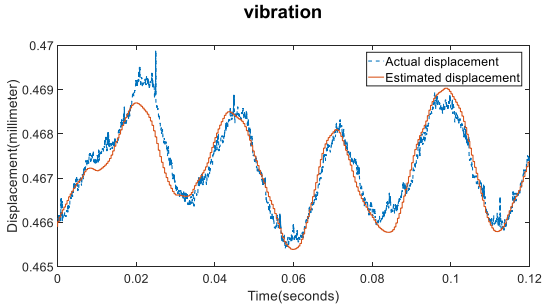

FIGURE 17. Displacement comparison of radial bearing under 1000 Hz vibration.

The system parameters are shown in Table 2.

In order to verify the accuracy of the designed displacement estimation algorithm, the coil currents of the radial bearing AX under sinusoidal vibration of 100 Hz, 500 Hz, and 1000 Hz are taken as the input of the designed displacement estimation method in this paper. And system control algorithm is incomplete derivative PID control [27]. The estimated displacement is compared with the actual displacement, and the data acquisition frequency are 100 kHz, as shown in Figs. 15-17.

It can be seen from Fig. 15 that when the rotor of the magnetic bearing motor runs stably and vibrates sinusoidally, the designed algorithm can effectively follow the actual displacement. It also can be seen from Fig. 16 and Fig. 17 that even if the magnetic bearing motor is disturbed, the rotor is not sinusoidally vibration, the designed algorithm can still follow the actual displacement. The deviation of estimated displacement and actual displacement of the designed method are shown in Table 3.

It can be seen from Table 3 that in the case of a radial magnetic bearing gap of 0.5 mm, the maximum deviation rate does not exceed 1%, which is the deviation that the magnetic bearing system can withstand for stable operation. The experimental results show that the method proposed in this paper can realize the sensorless operation of the magnetic bearing system.

TABLE 2. Magnetic bearing motor parameters.

The motor power	250kW
Bus voltage	110V
The quality of rotor	70kg
Switching frequency	20kHz
Pole face area	1150mm^2
Radial coil turns,	230N
Nominal air gap	0.5mm

TABLE 3. Comparison with actual displacement.

Vibration Frequency /Hz	Maximum Deviation /mm	Maximum deviation rate
100	0.0043	0.86%
500	0.0011	0.22%
1000	0.0019	0.38%

VI. CONCLUSION

In this paper, a self-sensing magnetic bearing displacement estimation algorithm based on BSW is designed, and a magnetic bearing system model and displacement estimator are built in the Matlab Simulink environment. The simulation compares and analyzes the Fourier analysis method considering the duty cycle and the designed BSW algorithm. The simulation results show that the designed multiresolution filter bank biorthogonal spline wavelet algorithm overcomes the Gibbs effect and reduces the influence of ripple on the rotor displacement estimation when the magnetic bearing motor operates within 1 kHz. The stability has been improved by 38%, and the accuracy has been improved by 35%, and the effectiveness of the proposed displacement estimation method is proved on the magnetic bearing experimental platform.

REFERENCES

[1] Y. Jie and Z. Changsheng, "Self-sensing active magnetic bearing using Hilbert transform," *J. ZheJiang Univ. (Eng. Sci.)*, vol. 49, no. 4, pp. 732–739, 2015.

[2] Y. Jiang, X. Ma, and Y. Fan, "Rotor displacement self-sensing approach for permanent magnet biased magnetic bearings using double-axis PWM demodulation," *IEEE Sensors J.*, vol. 18, no. 19, pp. 7932–7940, Oct. 2018.

[3] T. Zhang, X. Liu, L. Mo, X. Ye, W. Ni, W. Ding, J. Huang, and X. Wang, "Modeling and analysis of hybrid permanent magnet type bearingless motor," *IEEE Trans. Magn.*, vol. 54, no. 3, pp. 1–4, Mar. 2018.

[4] G. Schweitzer and H. Eric Maslen, *Magnetic Bearings: Theory, Design, and Application to Rotating Machinery*. Beijing, China: China Machine Press, 2009.

[5] J. Yu, X. Wu, Y. Zhang, J. Li, and R. Ni, "A novel differential estimation method of rotor displacement for active magnetic bearings," in *Proc. 22nd Int. Conf. Electr. Mach. Syst. (ICEMS)*, Aug. 2019, pp. 1–5.

[6] T. Liu, H. Zhu, M. Wu, and W. Zhang, "Rotor displacement self-sensing method for six-pole radial hybrid magnetic bearing using mixed-kernel fuzzy support vector machine," *IEEE Trans. Appl. Supercond.*, vol. 30, no. 4, pp. 1–4, Jun. 2020.

[7] D. Vischer and H. Bleuler, "A new approach to sensorless and voltage controlled AMBs based on network theory concepts," in *Proc. 2nd Int. Symp. Magn. Bearings*, Tokyo, Japan, 1990, pp. 301–306.

[8] D. Vischer, "Sensorlose und spannungsgesteuerte magnetlager," M.S. thesis, Swiss Federal Inst. Technol., Zürich, Switzerland, 1988.
[9] D. Vischer and H. Bleuler, "Self-sensing active magnetic levitation," *IEEE Trans. Magn.*, vol. 29, no. 2, pp. 1276–1281, Mar. 1993.
[10] H. Bleuler, "A survey of magnetic levitation and magnetic bearing types," *JSME Int. J. III, Vibrat., Control Eng., Eng. Ind.*, vol. 35, no. 3, pp. 335–342, 1992.
[11] N. M. Thibeault and R. S. Smith, "Magnetic bearing measurement configurations and associated robustness and performance limitations," *J. Dyn. Syst., Meas., Control*, vol. 124, no. 4, pp. 589–598, Dec. 2002.
[12] M. Tang and C. Zhu, "New method of position estimation for self-sensing active magnetic bearings based on artificial neural network," in *Proc. Int. Conf. Electr. Control Eng.*, Jun. 2010, pp. 1355–1358.
[13] G. van Schoor, A. C. Niemann, and C. P. du Rand, "Evaluation of demodulation algorithms for robust self-sensing active magnetic bearings," *Sens. Actuators A, Phys.*, vol. 189, pp. 441–450, Jan. 2013.
[14] J.-S. Yim, S.-K. Sul, H.-J. Ahn, and D.-C. Han, "Sensorless position control of active magnetic bearings based on high frequency signal injection with digital signal processing," in *Proc. 19th Annu. IEEE Appl. Power Electron. Conf. Expo. (APEC)*, Feb. 2004, pp. 1351–1354.
[15] P. Garcia, J. M. Guerrero, I. El-Sayed, F. Briz, and D. Reigosa, "Carrier signal injection alternatives for sensorless control of active magnetic bearings," in *Proc. 1st Symp. Sensorless Control Electr. Drives*, Jul. 2010, pp. 78–85.
[16] Z. Zhu, M. Dai, L. Zeng, J. Sun, and Y. Zhang, "Research on testing principle of self-sensing magnetic bearing system," in *Proc. 4th Int. Conf. Control, Autom. Robot. (ICCAR)*, Apr. 2018, pp. 301–304.
[17] D. Rui, "Research on rotor position self-sensing and power amplifiers of active magnetic bearings," M.S. thesis, Wuhan Univ. Technol., Wuhan, China, 2006.
[18] J. Chaowu and X. Longxiang, "Differential transformer displacement sensors and application in active magnetic bearings," *J. Mech. Eng.*, vol. 45, no. 11, pp. 78–84, 2009.
[19] M. D. Noh and E. H. Maslen, "Position estimation in magnetic bearings using inductance measurements," in *Proc. Magn. Bearings Ind. Conf.*, 1995, pp. 249–256.
[20] T. Ming and Z. Changsheng, "Research of self-sensing active magnetic bearings based on duty cycle compensation," *J. ZheJiang Univ. (Eng. Sci.)*, vol. 47, no. 8, pp. 1418–1423, 2013.
[21] J. Yu and C. Zhu, "Self-sensing active magnetic bearing using wavelet based position estimation algorithm," in *Proc. 17th Int. Conf. Electr. Mach. Syst. (ICEMS)*, Oct. 2014, pp. 748–751.
[22] T. Ming, Z. Changsheng, and Y. Jie, "Cooperative rotor position estimation of active magnetic bearings with unsaturated magnetic bias," *Trans. China Electrotech. Soc.*, vol. 29, no. 5, pp. 205–212, 2014.
[23] Y. Jie, Z. Changsheng, and Y. Zhonglei, "Rotor position estimation strategy for self-sensing active magnetic bearing considering eddy currents," *Trans. China Electrotech. Soc.*, vol. 33, no. 9, pp. 1946–1956, 2018.
[24] T. Liu and Y. Wu, "Multimedia image compression method based on biorthogonal wavelet and edge intelligent analysis," *IEEE Access*, vol. 8, pp. 67354–67365, 2020.
[25] Y. Sun, J. Xu, H. Wu, G. Lin, and S. Mumtaz, "Deep learning based semi-supervised control for vertical security of maglev vehicle with guaranteed bounded airgap," *IEEE Trans. Intell. Transp. Syst.*, pp. 1–12, 2021.
[26] C. Wang, Z. Wang, L. Zhang, D. Cao, and D. G. Dorrell, "A vehicle rollover evaluation system based on enabling state and parameter estimation," *IEEE Trans. Ind. Informat.*, vol. 17, no. 6, pp. 4003–4013, Jun. 2021.
[27] M. Lahdo, T. Strohla, and S. Kovalev, "Design and implementation of an new 6-DoF magnetic levitation positioning system," *IEEE Trans. Magn.*, vol. 55, no. 12, pp. 1–7, Dec. 2019.

HAOJIE XIONG was born in Chengdu, China. He is currently pursuing the master's degree in electrical engineering with Northeastern University, Shenyang, China. His research interests include active magnetic bearings, wavelet transforms, and displacement sensor-less technology.

JUN XIAO received the B.S., M.S., and Ph.D. degrees from Northeastern University, China, in 1989, 1992, and 2001, respectively. From 2002 to 2003, she was a Visiting Scholar with Michigan State University, East Lansing, MI, USA, where she worked on the control of micro wall-climbing robots. She is currently an Associate Professor with the College of Information Science and Engineering, Northeastern University. Her research interests include robotics, sensor networks, intelligent control, and fuzzy control.

DONGSHENG YANG (Senior Member, IEEE) was born in Fushun, China. He received the B.S. degree in testing technology and instrumentation, the M.S. degree in power electronics and electric drives, and the Ph.D. degree in control theory and control engineering from Northeastern University, Shenyang, China, in 1999, 2004, and 2007, respectively. He was with Northeastern University as a Lecturer for one year and an Associate Professor for three years, where he is currently a Professor. His research interests include magnetic bearings, electromechanical equipment, control engineering, fault diagnosis, and multi-energy power systems. He is the General Secretary of IEEE PES China Transformers Satellite Committee-China. He is selected as the Distinguished Professor of Liaoning Province and the New Century Excellent Talents of Education Ministry of China. He is also the Director of the Energy Interconnection Equipment and Technology Committee of China Machinery Federation. He received the Second Prize of the National Science and Technology Progress, in 2010, and the First Prize of the Science and Technology Progress of Chinese Association of Automation, in 2020.

BOWEN ZHOU (Member, IEEE) received the B.Sc. and M.Sc. degrees in electrical engineering from Wuhan University, Wuhan, China, in 2010 and 2012, respectively, and the Ph.D. degree in electrical engineering from Queen's University Belfast, Belfast, U.K. In 2016, he joined the College of Information Science and Engineering, Institute of Electric Automation, Northeastern University, Shenyang, China, where he is currently working as a Lecturer. He is the PI or Co-I of more than ten government or industry sponsored projects. He has published more than 60 SCI or EI indexed articles. His research interests include power system operation, stability and control, vehicle to grid, energy storage and virtual energy storage, demand response, renewable energy, and energy internet. He is currently a member of IET, IAENG, CSEE, CAA, and CCF. He is also a standing director or director of several IEEE PES China committees and subcommittees. He has served as a session chairs and a TC/PC members for more than ten international conferences.

XIAOTING GAO (Graduate Student Member, IEEE) was born in Shenyang, China. She received the B.S. degree in electronic information engineering and the M.S. degree in electrical engineering from the Shenyang University of Technology, Shenyang, in 2013 and 2016, respectively. She is currently pursuing the Ph.D. degree in electrical engineering with Northeastern University, Shenyang. Her research interests include active magnetic bearing, control engineering, and power quality monitoring. She is a Committee Member of IEEE PES Transformers Satellite Committee-China. She received the First Prize of Science and Technology Progress of Chinese Association of Automation, in 2020.